Rapid Thiol-Yne-Mediated Fabrication and Dual Postfunctionalization of Micro-Resolved 3D Mesostructures

Alexander S. Quick, Andres de los Santos Pereira, Michael Bruns, Tiemo Bückmann, Cesar Rodriguez-Emmenegger, Martin Wegener,* and Christopher Barner-Kowollik**

3D mesostructures with a height of up to 1 mm and micrometer feature size are fabricated employing a writing speed of 1 cm s^{-1} via direct laser writing utilizing a novel functional photoresist based on the radical coupling reaction of thiols and alkynes. The refractive index of the resist—consisting of a tetrafunctional thiol, a tetrafunctional alkyne and a photoinitiator—is tailored to be compatible with the employed high numerical aperture (NA) objective lens, thus enabling a Dip-in configuration. Mesostructures are characterized by scanning electron microscopy, optical photography, and nondestructive 3D time-of-flight secondary ion mass spectrometry. Woodpile photonic crystals are fabricated as benchmark structures in order to investigate the axial resolution. Verification of the chemical fabrication mechanism is achieved via transmission Fourier transform infrared (FTIR) spectroscopy of fabricated cuboid structures by monitoring the decrease of corresponding thiol and alkyne absorption peaks. Postmodification reactions, namely the thiol-Michael addition and the copper-catalyzed azide alkyne cycloaddition, are conducted employing residual thiols and alkynes throughout the cuboid structures. Successful dual and orthogonal modification throughout the structure and on the surface is achieved and verified utilizing transmission FTIR spectroscopy and time-of-flight secondary ion mass spectrometry.

1. Introduction

Materials science has evolved into a central research field as it enables accessing materials with new properties as well as highly specific functions. It concomitantly aims at gaining mechanistic knowledge of the processes, underpinning the macroscopically observable properties. Rapid progress in top-down and bottom-up design approaches have led to new ways to engineer materials in the micro and nanometer range. Driven by a strong interest in the area of functional microengineering, a plethora of techniques for a large variety of materials has been established in order to achieve an ever finer control over structure and function. While some techniques aim at the fabrication, modification, and self-assembly of micro- and nanoparticles by exploiting microfluidics, lithography, and wet-chemical processes,[1–4] other techniques such as atomic layer deposition or the self-assembly of monolayers allow for surface engineering.[5,6] High lateral resolution for 2D structuring can be obtained via nanoimprint techniques or electron-beam lithography.[7,8] The latter additionally allows for the limited fabrication of 3D structures.[9] With increasing technological advances, the complexity and availability of materials has also been drastically increased. Although most of the employed techniques are rather specific and thus are applied for one certain application, other tools have recently emerged which can be more generally applied. One such tool for the fabrication of versatile, almost arbitrary 3D micro- and nanostructures is direct laser writing

T. Bückmann, Prof. M. Wegener
Institute for Applied Physics (APH)
and Center for Functional Nanostructures (CFN)
Karlsruhe Institute of Technology (KIT)
Wolfgang-Gaede-Strasse 1, 76131 Karlsruhe, Germany
E-mail: martin.wegener@kit.edu

A. S. Quick, Prof. C. Barner-Kowollik
Preparative Macromolecular Chemistry
Institut für Technische Chemie und Polymerchemie (ITCP)
Karlsruhe Institute of Technology (KIT)
Engesserstrasse 18, 76131 Karlsruhe, Germany
E-mail: christopher.barner-kowollik@kit.edu

A. S. Quick, Prof. C. Barner-Kowollik
Institut für Biologische Grenzflächen (IBG)
Karlsruhe Institute of Technology (KIT)
Hermann-von-Helmholtz-Platz 1
76344 Eggenstein-Leopoldshafen, Germany

DOI: 10.1002/adfm.201500683

A. de los Santos Pereira,
Dr. C. Rodriguez-Emmenegger
Institute of Macromolecular Chemistry
Academy of Sciences of the Czech Republic v.v.i.
Heyrovsky sq. 2, 162 06 Prague, Czech Republic
E-mail: rodriguez@imc.cas.cz

Dr. M. Bruns
Institute for Applied Materials (IAM)
Karlsruhe Nano Micro Facility (KNMF)
Karlsruhe Institute of Technology (KIT)
Hermann-von-Helmholtz-Platz 1 76344
Eggenstein-Leopoldshafen, Germany

(DLW).[10–13] In DLW, essentially, a femtosecond pulsed laser beam is tightly focused into a photoreactive resist. In the confined focus, curing of the resist occurs via a nonlinear absorption mechanism. By scanning either the focus and the stage or only the stage 3D structures are fabricated. While the preparation of structures remains similar, different architectures can be implemented for a multitude of different applications ranging from microdevices,[14] lab-on-a-chip systems,[15] and confinement of cells to specific microenvironments[16] to optical and mechanical metamaterials.[17,18]

An important reason for the above mentioned versatility of DLW is the continuous refinement and improvement of the technique throughout the last decade. A critical parameter for the production of large structures is the writing speed as it drastically reduces the overall fabrication time. During a typical DLW routine, the stage is moved using piezoelectric actuators while the focus remains stationary. Due to mechanical issues occurring during acceleration and deceleration of the stage during fabrication, the speed is limited to about 100–200 μm s^{-1}. The use of galvo-mirrors has been exploited to increase the writing speed.[19] In this configuration the stage remains stationary on the horizontal axes. The writing in each plane is performed by rapid scanning of the area conducted via moving of the galvo-mirror set, i.e., moving of the focused beam. The vertical movement remains stage controlled and the writing procedure occurs in a layer-by-layer manner, enabling writing speeds of up to several cm s^{-1}, exceeding the obtainable speed for piezoelectric actuator-driven DLW by a factor of approximately 100.

In conventional DLW, the laser beam passes through immersion oil and the glass cover-slip before curing in the photoresist occurs.[20] This facile approach is very versatile as it allows a broad choice of the photoresist and other deviations for lithographic applications and has therefore been established as the standard method for DLW. However, this method poses serious constraints to the maximum achievable heights and requires substrates that are transparent to the laser beam. The height limitation results from the given working distance of the objective. Furthermore, refractive-index (RI) mismatches between the substrate and the photoresist/structure impair the quality of fabricated parts with increasing distance from the interface of the coverslip. Although the problem of substrate transparency can be circumvented by extensions to the standard method, the height limitation remains.[21] To overcome this obstacle, Dip-in DLW has recently been developed.[22] In this method, the objective is directly immersed into the photoresist during the lithographic process. A prerequisite hereby is a compatible RI of the liquid photoresist for the lens of the utilized high numerical aperture objective. Thus, depth-dependent aberrations and the working distance no longer limit the accessible dimensions, enabling—together with fast scanning speeds—mesoscopic structures with micro/nanometer scale feature size.[18] These benefits are, however, accompanied by the need of compatible refractive indices between the objective lens and the liquid photoresist.

A further challenge DLW needs to face for extending its use to other fields is the ability to precisely postmodify written structures. Many conceivable applications of structures ranging from biosensing and nanomechanobiology to diagnostics and microfluidics require that the generated structures are functionalized by chemical means throughout the volume and on the surface. To be more specific, chemical control is highly important regarding the biocompability and controlled immobilization of specific biomolecules. Further, the controlled covalent introduction of catalysts, detector molecules or any other beneficial or even crucial chemical moiety for a specific application is highly desired. A success in the functionalization of complex and intricate structures requires highly efficient chemical reactions such as those based on spring-loaded click chemistries.[23] So far, advances in DLW have been mainly focused on physics and engineering of the method while chemical improvement has been—to a large extent—dominated by free radical and cationic polymerization methodologies. Alongside other interesting investigations, for instance concerning the implementation of hybrid materials to DLW, photofixation in Diels–Alder networks and DLW surface functionalization in a multistep approach,[24–26] our team has recently established novel photoresists exploiting different polymerization protocols by employing radical thiol-ene and light-induced Diels–Alder chemistry (photoenols).[27,28] By utilizing these chemistries, the resulting structures can directly be covalently modified via two chemical pathways: by thiol-Michael addition reaction or by the Diels–Alder reaction, the latter enabling spatially resolved functionalization. However, further important methods such as a facile dual functionalization via two orthogonal chemistries cannot be achieved employing the above noted pathways. In order to address these challenges, it is important to investigate novel systems to further enlarge the possibilities of precision postmodification.

Radical thiol-yne coupling (TYC) has recently gained increased attention in the course of the click chemistry paradigm.[23] In this reaction, thiyl radicals are generated, commonly via usage of a photoinitiator.[29–31] In the presence of alkynes, a covalent sulfur–carbon bond together with a vinyl radical is generated. After hydrogen transfer from an additional thiol, a vinyl sulfide and another thiyl radical are produced. Additionally, vinyl sulfides are also susceptible to reaction with thiyl radicals via thiol-ene coupling (TEC), ultimately affording bis-sulfide species. In comparison to TYC, TEC reactions possess even higher radical addition coefficients.[32] Strictly speaking, TYC does not fulfill some important click chemistry criteria concerning stereoselectivity or the formation of one sole product. By using multifunctional alkyne and thiol species, however, this reaction enables the facile production of highly crosslinked and uniform polymeric networks.[33] The rapid network formation makes TYC an ideal chemistry for the generation of functional and addressable DLW structures. Furthermore, the mentioned polymerization technique allows for tailoring of resulting polymeric materials. For instance, the sulfur content can be exploited for precise tailoring of network parameters such as the RI and the density.[34]

Here, we present a novel photoresist system for 3D DLW lithography consisting of a tetrafunctional thiol, a tetrafunctional alkyne, and a photoinitiator. Curing of the resist in the fabrication step is achieved by triggering TYC obtaining insoluble, highly crosslinked uniform polymeric structures (see **Figure 1**). The RI of the uncured resist is tailored concerning the number of sulfur atoms. Consequently, Dip-in DLW can be performed, enabling the fabrication of high structures (≈1 mm)

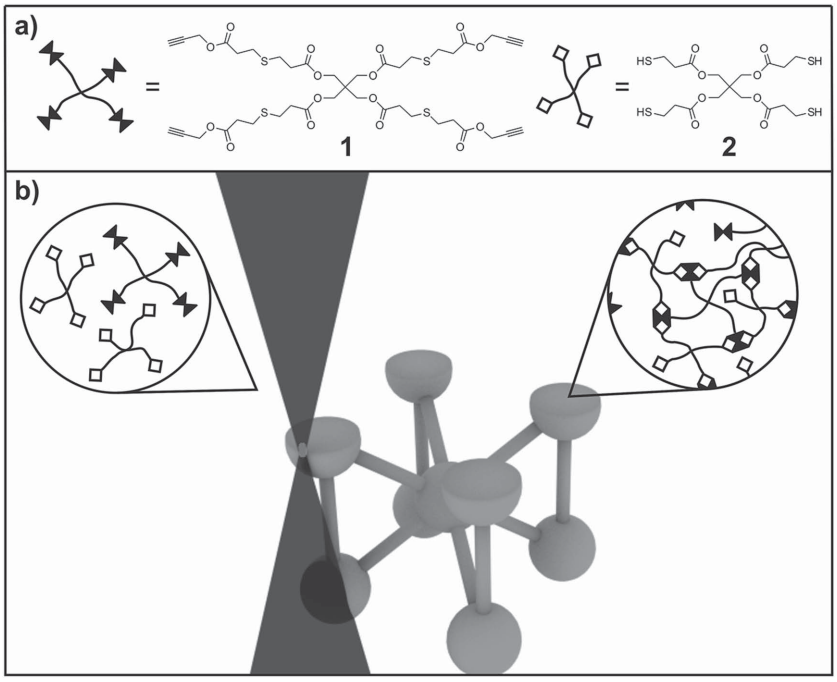

Figure 1. a) Schematic and chemical depiction of both main components of the thiol-yne photoresist: the tetrafunctional alkyne (**1**) and the tetrafunctional thiol (**2**) (ratio: 1:2). b) Schematic depiction of the photoresist in uncured (left) and cured (right) regions during a DLW experiment with functional groups as lock-and-key models. The reaction of each alkyne with two thiols in total (via the vinyl sulfide) is indicated by the double lock shape of the alkyne.

that are not accessible by the standard oil-immersion approach. Rapid writing speeds of 1 cm s^{-1} are utilized, enabling the fabrication of complex mesoscopic 3D objects with micrometer scale feature sizes. Resulting structures are monitored by a high-resolution camera, scanning electron microscopy (SEM) and time-of-flight secondary ion mass spectrometry (ToF-SIMS). Further, the axial resolution of the photoresist is investigated by fabrication and characterization of woodpile photonic crystals as benchmark structures. The postulated chemical reactions proceeding during the fabrication step are verified by tracing of the alkyne and the thiol vibrational bands employing transmission FTIR spectra of generated cuboid structures. Furthermore, transmission FTIR analysis reveals the existence of residual thiols and alkynes throughout the structure after fabrication. In further steps, the aforementioned functional groups are exploited as components in corresponding click reactions, i.e., the thiol-Michael addition reaction and the copper-catalyzed azide alkyne cycloaddition (CuAAC), allowing for the dual postmodification of fabricated DLW structures via both click reactions. Successful dual postwriting modification reactions were verified throughout the structure and on the surface utilizing FTIR spectroscopy and ToF-SIMS, respectively. The new system can be seen as a potent, easy to handle resist platform that can be employed for a multitude of applications.

2. Photoresist Design

Although different photoresists have been introduced to DLW over the past decade, many beneficial features frequently employed for materials science have not yet been met. For instance, facile dual postfunctionalization of fabricated structures largely improves the range and flexibility of structural tailoring. Therefore, the development of novel photoresists is important in order to meet such challenges. Typical considerations for formulating a resist are a) ease of preparation of the final resist as well as the synthesis of components, b) compatibility with the most recent DLW innovations which are not necessarily based on resist development, and finally c) introduction of new or improvement of existing features concerning, e.g., structure fabrication or postmodification. In the current study, we introduce the radical coupling between alkynes and thiols as a curing reaction for DLW driven microstructure fabrication. The resist consists of three components, a tetrafunctional alkyne (**1**), a tetrafunctional thiol (**2**), and a photoinitiator (7-diethlamino-3-thenoylcoumarin). Both the thiol and the initiator are commercially available, while the alkyne can be readily synthesized (see the Experimental Section and Figure S1, Supporting Information). Thiol and alkyne components are mixed in a ratio of 2:1 based on the molarity of the functional groups. This ratio takes into account that the intermediate vinyl sulfide undergoes a radical TEC with another thiol, a reaction that was shown to be faster than its thiol-yne counterpart.[32,35] Therefore, it can be assumed that the majority of vinyl sulfides react during DLW exposure. A photoinitiator is added in a small quantity, enabling the generation of radical species in the absorption volume that is required for the reaction. Due to the intermediate vinyl sulfide species, TYC with monofunctional molecules leads to the formation of hyperbranched species. Combined with the usage of tetrafunctional starting molecules this method leads to the formation of stable, densely crosslinked polymer networks. Since the two main components are miscible and small amounts of photoinitiator are soluble therein, the resist does not require any addition of solvents which are often needed in order to obtain homogeneous liquid resists. Solvent-associated drawbacks such as evaporation during fabrication leading to a change of threshold power, the precipitation of components or even the complete desiccation of the sample do not occur in the resist presented here, hence greatly facilitating structure fabrication. In addition—while it is possible to freshly prepare resists before usage—a long shelf life is highly desirable, especially for research that requires a great number of identical samples over a longer period of time. The resist presented in the current study was stored at ambient conditions in the dark. Samples for lithography experiments were withdrawn under yellow light conditions displaying no visible alteration of the photoresist performance over a period of up to one month whereupon the mixed batch was entirely consumed. In principle, a wide range of different thiols and alkynes can be considered as resist components allowing for facile photoresist tailoring and making

thiol-yne-mediated DLW attractive for several lithography-connected applications.

One of the main foci of the present work is to combine the thiol-yne resist with the above mentioned DLW improvements, enabling the facile fabrication of high structures employing fast writing speeds. Therefore, the photoresist was tailored in a manner such as to make it compatible with Dip-in DLW. This process requires adjusting the photoresist RI for the high NA objective lens. A compatible RI for the employed objective is 1.52 at 23 °C and 589 nm (values are taken from commercially available immersion oil). One possibility to tailor the RI of the photoresist is by adjusting the sulfur content. In general, increased sulfur content leads to an increased RI. The tetraalkyne (**1**) was therefore chosen such as to also include sulfur atoms. Thus, the employed photoresist features an RI of 1.52 (23 °C, 589 nm) which is compatible with the employed objective, enabling convenient usage of the photoresist for fabrication of mesostructures.

3. Structure Fabrication and Characterization

In order to demonstrate the lithographic possibilities that can be achieved with the new photoresist, demanding parameters were selected to assess its performance. The maximum specified writing speed of the setup (1 cm s^{-1}) via the usage of galvo-mirrors was utilized for the experiments while keeping the writing power at 21 mW and the slicing distance of the layers at 0.4 µm. The precise RI tuning of the resist allowed for lithography experiments in Dip-in configuration. Fabrication in this configuration enables facile access to mesoscopic objects with micrometer scale feature size. In order to verify this, a range of structures were fabricated in this study consisting of body-centered cubic unit cells (see Figure S2 in the Supporting Information). While each period consisted of an array of 4×4 unit cells, the number of periods in axial direction was varied. That way structures with 1, 2, 4, 8, and 32 periods were subsequently fabricated in one single lithographic step. The nominal lateral dimension of each layer was set to be 132.5 μm^2. The nominal height of each structure was set to be 42.5, 72.5, 132.5, 252.5, and 972.5 µm, respectively. The tallest structure consisting of 32 periods of unit cells was investigated in more detail (see **Figure 2**). SEM images of the entire structure as well as close-up views from the top and the side revealed a uniform, fully resolved structure with a smooth surface and only sparse deformation. From Figure 2a, the height of the structure was calculated to be close to 970 µm (the angle of the stage was set to be 45°). The small difference between the nominal and calculated height confirmed the high structure quality. Since the 32-period mesoscopic structure is easily visible to the eye, it could also be imaged with a camera (see **Figure 3**a). For comparison, a screw with a diameter of 2 mm (including the winding) was placed in the background. In addition, a third method that is rather uncommon for nondestructive 3D structure characterization was utilized.

Characterization containing chemical information of well-defined intricate 3D structures is a challenging task. To improve the range of applicable methods, we introduced the use of ToF-SIMS for DLW structure characterization. Although the ToF-SIMS technique is usually exploited for characterization of

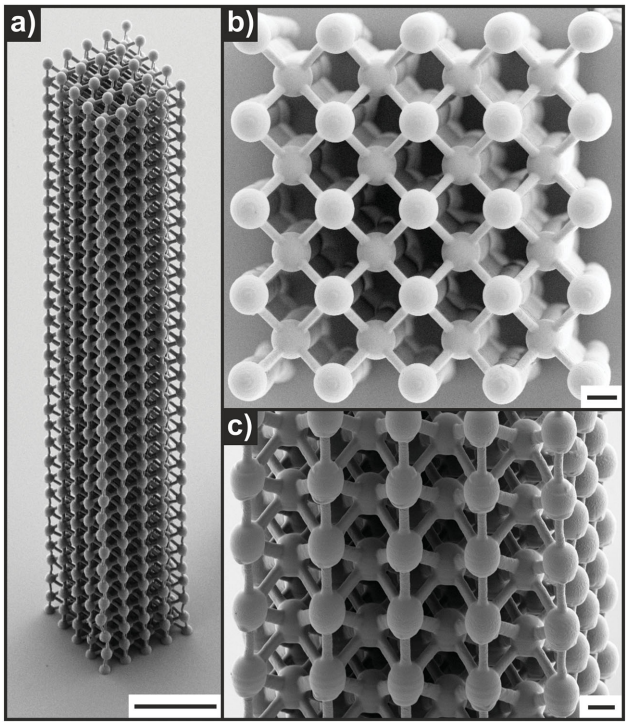

Figure 2. SEM analysis of the tallest fabricated structure consisting of 32 layers of 4 × 4 body-centered cubic unit cells with a nominal height of 972.5 µm. Part (a) depicts the entire structure while parts (b) and (c) are close-up views of the top and the side of the structure, respectively. The analysis reveals a uniform, 3D mesoobject with micrometer feature size exhibiting a smooth surface. Scale bars are 100 µm for (a) and 10 µm for (b) and (c).

2D or, via sputter-depth profiling, 3D systems we extended its limits for the nondestructive analysis of 3D objects. For demonstration purposes, a gold coated structure with four periods was characterized by ToF-SIMS analysis (see Figure 3b,c) after conventional SEM imaging (see Figure S3 in the Supporting Information). The depicted total ion count and Au^- images display the 3D structure in a good quality and resolution, clearly demonstrating ToF-SIMS analysis as a suitable technique for efficient, mild, and nondestructive 3D characterization with the advantage to achieve chemical/molecular information simultaneously. While the analysis of the gold coated structure served as a proof of principle, the here described configuration is utilized for the investigation of surface bound moieties later in this study. Together, the utilized characterization methods clearly show that mesoscopic objects with micrometer scale feature sizes can be rapidly fabricated using this resist, taking full advantage of state-of-the-art DLW innovations.

Another important parameter for novel 3D lithographic systems is the achievable axial resolution. For this purpose, woodpile photonic crystals were fabricated and investigated as complex 3D benchmark structures.[36] As fixed parameters, a writing speed of 1 cm s^{-1}, a footprint of 50 μm^2, a total number of 10 periods (40 layers), a rod distance of 3 µm, and a layer distance of 1.13 µm were chosen while the laser power was varied. Subsequently, reflectance spectra for woodpiles produced at different powers were collected in order to investigate the corresponding

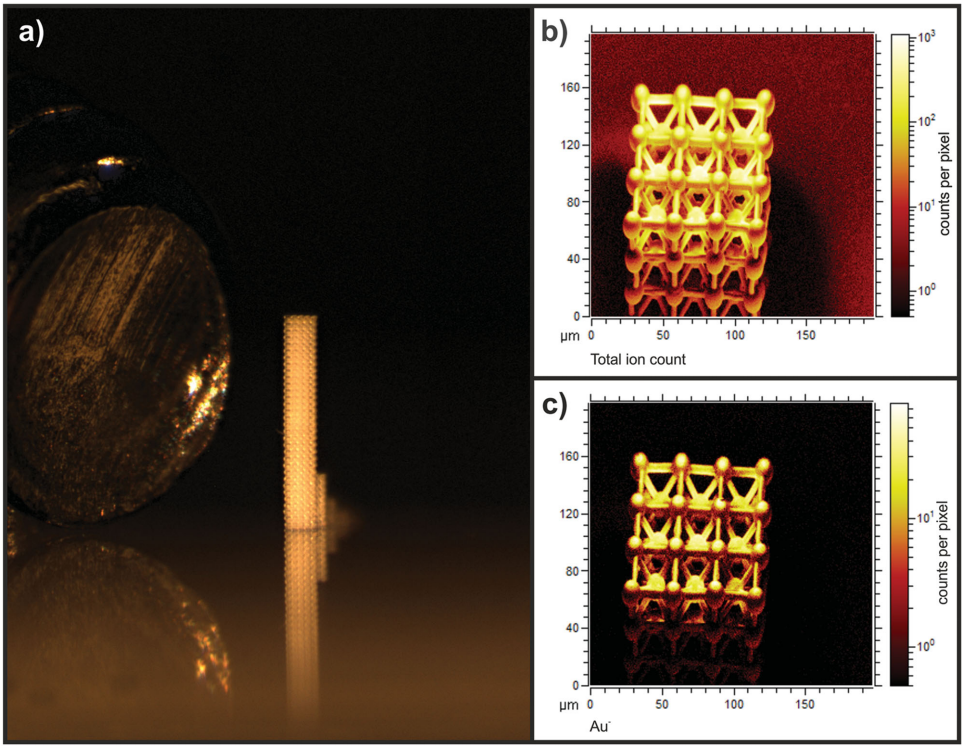

Figure 3. a) Camera image of DLW fabricated structures. In front: the tallest structure with a nominal height of 972.5 μm. Smaller structures are visible in the background. For comparison a screw with a diameter of 2 mm (including the winding) is placed in the background. b) Total ion count and c) Au^- ToF-SIMS analysis of a similar gold coated object consisting of four layers of 3 × 3 body-centered cubic unit cells including horizontal bars.

photonic stop bands (see Figure S4 in the Supporting Information). By comparing the different spectra it becomes clear that for high average laser powers during fabrication (27 mW) no stop band is visible, indicating that the corresponding structure is not resolved. At 23.76 mW a stop band can be assigned. For decreasing writing powers, the filling fraction of the woodpile also decreases, thereby shifting the corresponding stop band to lower wavelengths. The highest quality structure, derived from the height of the stop band, was obtained for a laser power of 19.44 mW (23% reflectance). In order to further verify the quality of the generated woodpile, SEM analysis and focused-ion-beam milling (FIB) were performed (see Figure S5 in the Supporting Information). Thereby the high structural quality was confirmed. The here achieved resolution is clearly worse than for other available acrylate or epoxy-based resists and high resolution techniques based on two photon fabrication at 405 nm, stimulated emission depletion or inhibition.[37–39] We speculate that the resolution for this system is limited by the choice of the monomer components and the resulting polymer conversion obtained during fabrication. An increase in conversion resulting in stable structures can be achieved by multiple exposure as performed herein, yet by doing so small feature sizes cannot be reached anymore. A change in the core of the components could greatly increase the rigidity of the produced network, thus increasing structural stability. This approach would reduce deformation during writing and development which proved to be a limiting parameter for highly resolved structure fabrication.

A further important aspect of the new resist is the verification of the postulated chemical reaction during the fabrication process. Evidence of TYC being the dominating reaction during fabrication of 3D structures can be obtained from FTIR analysis. Therefore, solid cuboids with a thickness of 15 μm and base dimensions of 50 μm^2 were utilized for transmission-mode FTIR measurements. Thiols as well as alkynes have characteristic vibrational bands enabling to unequivocally prove their presence or absence.[40] Thiols exhibit a specific stretching vibration at 2550–2600 cm^{-1}. Terminal alkynes display two stretching vibrations, one at 2100–2150 cm^{-1} and the other at 3275–3325 cm^{-1} corresponding to the carbon–carbon triple bond and the carbon–hydrogen bond, respectively. **Figure 4** depicts the FTIR spectra of each resist component (excluding the photoinitiator), the photoresist, and a fabricated cuboid structure. The spectrum of the tetrafunctional alkyne shows absorption bands corresponding to stretching vibrations of different saturated alkanes between 2800 and 3000 cm^{-1} and the characteristic vibrations visible at 2127 and 3277 cm^{-1} that can be assigned to the stretching vibration of the triple bond and the terminal carbon–hydrogen bond, respectively. The spectrum of the tetrafunctional thiol exhibits a clear absorption peak at 2567 cm^{-1} that can be assigned to the thiol stretching vibration. The photoresist is, apart from the photoinitiator, merely a mixture of the thiol and alkyne. Therefore, the corresponding FTIR spectrum contains—as expected—both thiol and alkyne bands. During the crosslinking process radicals are released that allow the TYC to proceed. As mentioned above, the intermediate vinyl sulfide reacts rapidly in a TEC resulting in bisulfide species formation—the overall process is therefore a combination of radical TYC and TEC. In the overall reaction thiols and alkynes are

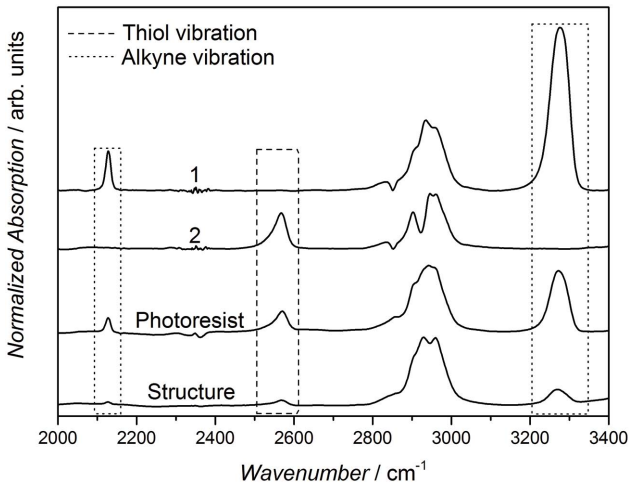

Figure 4. IR spectra of the tetrafunctional alkyne (**1**), the tetrafunctional thiol (**2**), the photoresist and a DLW fabricated, solid cuboid (from top to bottom). Distinct vibrations are detected at 2127 and 3277 cm^{-1} for the alkyne and at 2567 cm^{-1} for the thiol. The combined photoresist displays both alkyne and thiol bands. After fabrication, thiol and alkyne bands are clearly diminished, verifying the proposed curing mechanism yet also demonstrating the existence of residual functional groups after fabrication. For better clarity the spectra are shifted vertically.

consumed resulting in a significant decrease of their corresponding absorption peaks. By comparison of the photoresist and the spectrum of the written structure, the decrease is evident. Furthermore, the spectral data of the structure shows no significant band at slightly above 3000 cm^{-1}, characteristic for unsaturated bonds that are present in vinyl sulfides. Together, the spectra clearly reveal that the fabrication of structures proceeds via the proposed pathway. Importantly, it becomes clear that not all thiols and alkynes are consumed during the fabrication process. This finding is in agreement with the general mechanism of network formation. With increasing conversion the mobility of the participating molecules decreases. At some point the low mobility of the functional groups prevents further reaction. These residual functional groups therefore remain throughout the structure.

4. Covalent Postmodification

The verification of the proposed chemical pathway during the fabrication process evidenced the presence of residual thiols and alkynes throughout the structure which can be exploited in further postmodification strategies. Making use of these groups in highly effective reactions allows to finely tune the properties, for instance hydrophilicity or chemical functionality of the structures, while retaining the structural dimensions. Having the ability to tune properties of DLW-written structures is of key importance for extending their use into applications. In the present work, we exploited click reactions as a proof of concept for the dual surface modification via covalent bonds. Click reactions are well suited for this task as they combine an easy reaction procedure with orthogonality and hence versatility concerning different applications.

The residual thiols and alkynes throughout the structure are designated for the corresponding click reactions, namely thiol-Michael addition and CuAAC (see **Figure 5**a). For this purpose, DLW fabricated polymer cuboids were produced and subsequently modified (see Figure 5b and **Figure 6**a). After fabrication, the residual thiols were employed in a thiol-Michael addition reaction to immobilize a bromine-functional maleimide.

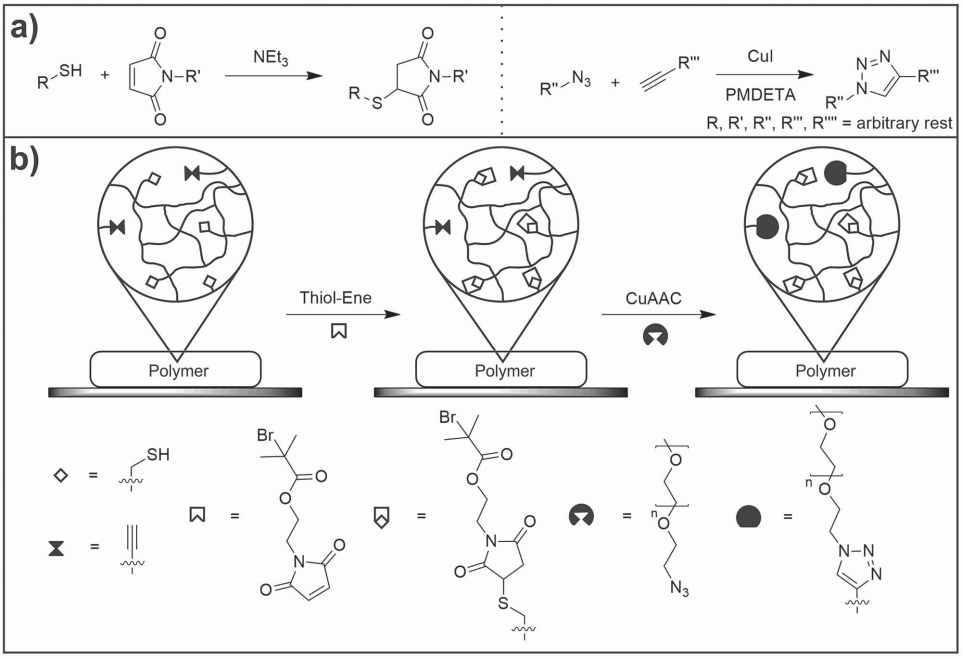

Figure 5. a) General description of both employed click reactions: the thiol-Michael addition reaction (left) and the CuAAC reaction (right). b) Schematic description of the postmodification reactions performed on DLW fabricated structures. In the first reaction, residual thiols throughout the structure are addressed in a thiol-Michael addition reaction. Subsequently, residual alkynes are reacted in a CuAAC reaction.

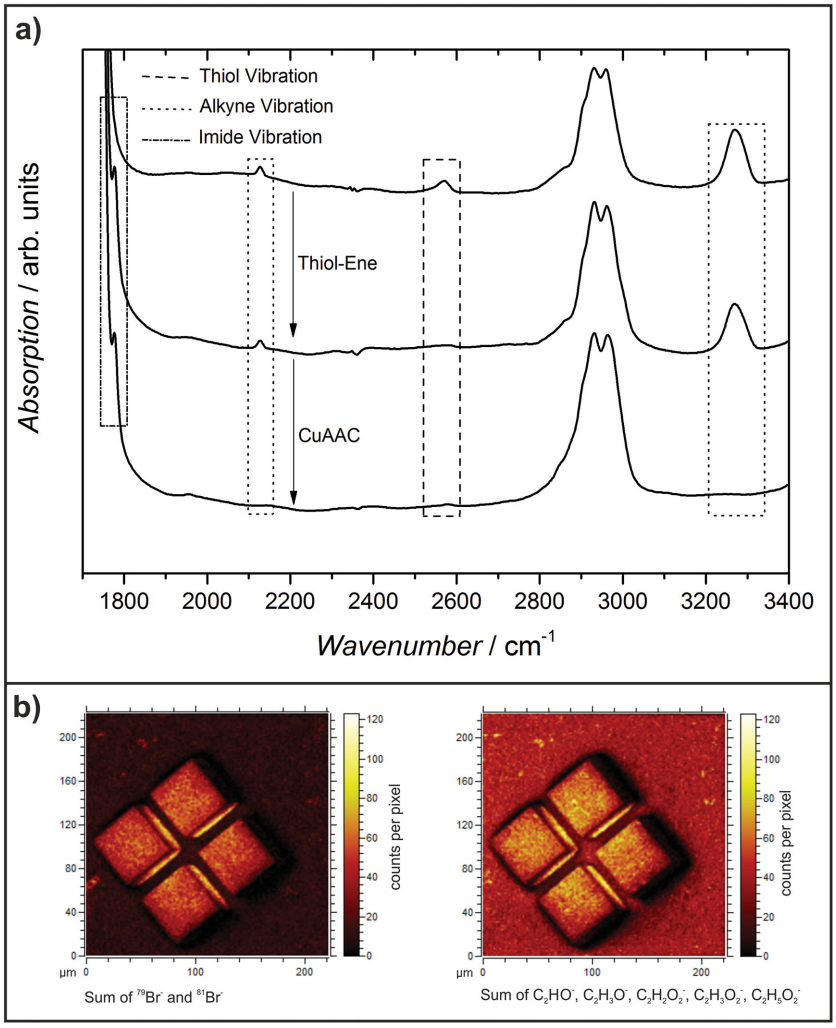

Figure 6. a) Verification of the postmodification reactions via IR spectroscopy (from top to bottom) throughout the cuboid structures. Absorption bands of residual thiols and alkynes are clearly visible in the spectrum of the fabricated sample (top). After the thiol-Michael addition reaction, the thiol absorption band is clearly decreased (middle). In addition, an absorption band corresponding to the imide is visible at 1776 cm^{-1}. Residual alkynes are addressed in a subsequent CuAAC reaction, verified by the decrease of the alkyne absorption bands (bottom). For better clarity the spectra are shifted vertically. b) ToF-SIMS analysis of the cuboid structures after thiol-Michael addition and subsequent CuAAC. The presence of bromine and PEG on the structural surface is evidenced via the sum of corresponding characteristic fragments, namely $^{79}Br^-$ and $^{81}Br^-$ (left) and C_2HO^-, $C_2H_3O_2^-$, $C_2H_2O_2^-$, $C_2H_3O_2^-$, and $C_2H_5O_2^-$ (right).

During this procedure, the cuboids were immersed into a solution containing the maleimide and a base in order to catalyze the reaction followed by a development step for the removal of nonbound species. FTIR spectra of the cuboids were collected before and after the thiol-Michael addition reaction. The collected spectra reveal that the residual thiols are consumed, evidenced by the clear diminution of the corresponding thiol band. Further, a saturated imide was covalently immobilized in the polymeric network stemming from the attached molecule. This alteration was clearly monitored in the FTIR spectra by an appearance of a band corresponding to the carbonyl vibration of the imide at 1776 cm^{-1}. The second band of the imide located at close to 1700 cm^{-1} cannot be taken as evidence for a successful functionalization due to the large overlap with other carbonyl vibrations. The thiol-Michael addition was orthogonal to the residual alkynes throughout the structure, indicated by the remaining absorption bands of the corresponding triple bonds. Therefore, subsequent to the thiol-Michael addition functionalization, the residual alkynes were employed for further covalent modification. Here, the alkyne groups were targeted by an α-azide poly(ethyleneglycol) methyl ether (PEG-N_3, M_n = 2000 g mol^{-1}) using a CuAAC reaction. The sample was immersed into a solution containing CuI, *N,N,N′,N″,N″*-pentamethyldiethylenetriamine (PMDETA), and PEG-N_3 to conduct the postfunctionalization reaction. Attaching large polymeric molecules to structures (grafting-to modification) is always challenging as it requires fast and efficient reactions. In a successful reaction alkynes are consumed, leading to a strong decrease of the corresponding absorption bands, clearly visible in the recorded spectra, and thus evidencing a successful reaction. While a distinct change for the alkyne bands is observed, the imide band remains unchanged in the spectra, serving as a good indication that the preceding thiol-Michael reaction product is not affected by the subsequent CuAAC reaction.

After evidencing the dual postmodification, it is important to further investigate the location of the functional groups. Although transmission FTIR spectroscopy reveals the success of each reaction, no information about the location of the covalently bonded molecules can be directly obtained. We speculate that the location of the residual functional groups after fabrication is randomly distributed within the 3D structure as neither the network formation nor the manner of fabrication channel the density of functional groups into a specific region. Therefore, a fraction of the residual functionalities must be located at the surface of the structure, an important feature as it increases the number of applications, e.g., in the field of biosensing or nanomechanobiology. Thus, cuboid structures functionalized via thiol-Michael addition and subsequent CuAAC were submitted to ToF-SIMS analysis (see Figure 6b). The molecules for covalent immobilization were chosen such as to exhibit characteristic fragments for characterization, namely a bromine or a PEG moiety for the thiol-Michael addition or CuAAC reaction product, respectively (see Figure 5b). From the ToF-SIMS analysis, a distinct bromine signal stemming from both isotopes ($^{79}Br^-$ and $^{81}Br^-$) is visible on the cuboid structures, revealing a successful attachment on the structural surface by the thiol-Michael addition reaction. Moreover, the viability of the thiol-Michael addition product for CuAAC reaction conditions is evidenced. Next to

the bromine fragments characteristic PEG fragments (C_2HO^-, $C_2H_3O^-$, $C_2H_2O_2^-$, $C_2H_3O_2^-$, and $C_2H_5O_2^-$) are revealed on the structures. Close observation of the PEG fragments in the ToF-SIMS image reveals that small quantities of PEG are also present next to the structures on the substrate surface which can be explained by unspecific adsorption. A reduction of this undesired effect could be achieved by changing the substrate or applying harsher development conditions. Nevertheless, analysis clearly shows the covalent immobilization of PEG on the structural surface, extending the evidence of successful dual functionalization to the structural surface. By combining two click reactions, a vast range of different molecules can be easily implemented into fabricated structures. Although the current study focuses on the proof of concept, the here attached molecules can, in principle, be employed for further scientific tasks. Via the thiol-Michael addition reaction a potent living radical polymerization initiator is implemented into the structure while with the CuAAC reaction PEG moieties are implemented that are often employed for bioapplications.

Both here employed click reactions proceed rapidly in solution and, given the correct conditions, can proceed to full conversion within minutes or even seconds. Thiol-Michael addition and CuAAC reactions performed in this study where conducted for 24 h or even 48 h, respectively. A shorter reaction time resulted in a less distinct change of the corresponding FTIR bands (not shown). This finding strongly indicates that the reaction rate of the chemical reactions is not the limiting factor in this approach but rather the diffusion of the components throughout the structure during postmodification.

In a different strategy, the order of the postmodification reactions was inversed, now starting with the CuAAC reaction. A structure was immersed in a solution of CuCl, PMDETA, and a chloride-containing azide (2-azidoethyl 2-chloropropanoate). Comparison of the FTIR spectra before and after the modification reaction evidenced the success of the reaction (see Figure S6 in the Supporting Information). Again the absorption bands for the alkyne decreased, confirming their consumption during the reaction. Unfortunately, also the thiol absorption band is strongly decreased indicating a consumption of thiols under the given conditions and thus impeding a subsequent thiol-Michael addition reaction. A possible explanation for this behavior is the usage of PMDETA. While it is employed as a ligand for the copper(I) complex in the CuAAC reaction, it also has the properties of a base and can therefore deprotonate and hence activate thiols. The activated species is a potent nucleophile that can possibly undergo side reactions. By comparing both sequential postmodification pathways, the possibility to straightforwardly obtain double covalent modification is restricted to the first pathway where the CuAAC reaction follows the thiol-Michael addition reaction.

5. Conclusions

Successful fabrication and postfunctionalization of 3D microstructures was demonstrated combining DLW with the radical TYC reaction. The novel photoresist, consisting of a tetrafunctional alkyne, a tetrafunctional thiol, and a photoinitiator, was carefully designed in order match the refractive index with respect to the objective lens, thus allowing for DLW in Dip-in configuration. Combined with the fast writing speeds enabled by galvo-mirrors, mesostructures with a height of close to 1 mm, and micrometer scale resolution were rapidly fabricated with a writing speed of 1 cm s^{-1}. Characterization of the structures was performed via SEM and a conventional camera, demonstrating good uniformity, quality, and a smooth surface. Furthermore, nondestructive ToF-SIMS was utilized for 3D structure imaging for—to the best of our knowledge—the first time. In addition, FTIR spectroscopy was performed on resist components, the photoresist and a cuboid structure verifying the postulated TYC during the fabrication process by observing a clear decrease of the corresponding thiol and alkyne absorption peaks. It was further shown that residual functional groups still existed throughout the structure due to the expected incomplete conversion during network formation. These residual functional groups were targeted for subsequent covalent postmodification reactions, namely the thiol-Michael addition reaction and the CuAAC reaction. Every reaction step was monitored by FTIR spectroscopy and ToF-SIMS analysis. By conducting the thiol-Michael addition reaction prior to the CuAAC reaction, a dual functionalization of the structure was achieved. Verification of the successful thiol-Michael reaction was evidenced by the strong decrease of the thiol absorption peak and the appearance of an imide carbonyl vibration deriving from the employed maleimide. The success of the azide-alkyne cycloaddition was verified by the strong decrease of the alkyne absorption bands after reaction. ToF-SIMS analysis confirmed the successful surface modification via both reactions by detecting characteristic fragments stemming from the attached molecules. The here presented photoresist combines the introduction of thiol-yne chemistry with most recent DLW innovations resulting in a simple to handle, rapid and powerful fabrication system. Combined with the possibility of a facile dual postmodification strategy, affecting both the bulk structure and the surface, the new resist system serves as a versatile platform for a range of different applications for instance in lab-on-a-chip systems, microfluidics, and microreactors.

6. Experimental Section

Materials: Pentaerythritol tetrakis(3-mercaptopropionate) (>95%, Sigma-Aldrich), propargyl acrylate (98%, Sigma-Aldrich), hexylamine (99%, Sigma-Aldrich), 7-diethylamino-3-thenoylcoumarine (DETC, Exciton), triethyl amine (99%, Acros Organics), acetone (99,5%, Roth), dimethylformamide (DMF, 99.5%, Acros Organics), dichloromethane (analytical grade, Fischer), copper(I) bromide (CuBr, 98%, Sigma-Aldrich), copper(I) chloride (CuCl, 97%, Sigma-Aldrich), PMDETA (99+%, Acros Organics), 3-(trimethoxysilyl)propyl methacrylate (98 %, Sigma-Aldrich), and methoxypolyethylene glycol azide (PEG-N_3, $M_n = 2000$ g mol^{-1}, Sigma-Aldrich) were used as received without further purification.

Synthesis of the Tetraalkyne Compound **1**: Compound **1** was synthesized employing a slightly modified literature procedure.[41] Pentaerythritol tetrakis(3-mercaptopropionate) (2.5 g, 5.12 mmol, 1 eq) and 30 µL of hexylamine was added to a round bottom flask. Under stirring, propargyl acrylate (2.5 g, 22.7 mmol, 1.1 eq) and was added over a period of 2 min. The mixture was stirred at ambient conditions for 1 h. Subsequently, residual propargyl acrylate and hexylamine was removed under reduced pressure. ^{1}H NMR (400 MHz, $CDCl_3$, δ): 4.70

(d, J = 2 Hz, 8H, CH_2), 4.16 (s, 8H, CH_2), 2.80 (m, 16H, CH_2), 2.65 (m, 16H, CH_2), 2.49 (t, J = 2 Hz, 4H, CH).

Synthesis of 2-Bromo-2-methyl Propionic Acid 2-(3,5-Dioxo-10-oxa-4-azatricyclo[5.2.1.02,6]dec-8-en-4-yl) Ethyl Ester: 2-Bromo-2-methyl propionic acid 2-(3,5-dioxo-10-oxa-4-azatricyclo[5.2.1.02,6]dec-8-en-4-yl) ethyl ester was synthesized employing a literature procedure.[42]

Synthesis of 2-Azidoethyl 2-Chloropropanoate: 2-Azidoethyl 2-chloropropanoate was synthesized employing a literature procedure.[43]

^{1}H NMR Spectroscopy: ^{1}H NMR spectroscopy was performed using a Bruker AM 400 spectrometer at 400 MHz. The δ-scale is referenced to the corresponding solvent signal.

Infrared Spectroscopy: Infrared spectroscopy was performed using a Bruker Tensor 27 Fourier-transform microscope spectrometer equipped with Hyperion 1000 unit. Spectra of the compound **1**, compound **2**, and the liquid photoresist were recorded employing attenuated total reflection infrared spectroscopy. Chemical analysis of the cuboid microstructures was performed via transmission IR spectroscopy using the Hyperion 1000 unit. Atmospheric compensation was performed upon the obtained transmission spectra. Woodpile photonic crystals analysis was performed via reflection IR spectroscopy using the Hyperion 1000 unit and a silver mirror as reference. The employed Cassegrain objective (Opticon 36x, NA = 0.5) illuminates the sample in an angular interval of 15°–30° from the optical axis. Spectra shown in Figure 4 were normalized via the highest peak in the region of 2900–2950 cm^{-1}.

Scanning Electron Microscopy: SEM imaging was performed using a Zeiss Supra 40VP. All samples were coated with a 7–10 nm gold layer prior to measurements.

Camera Imaging: Imaging was performed using a Sony GigE Vision XCG-500CR camera attached to a stereo microscope (Leica Mz 125 and a 0.5× adapter from Leica mount to C-mount).

Focused-Ion-Beam Milling: FIB was performed using a Zeiss Auriga equipped with a gallium ion source. The applied current was set to be 50 pA/30 kV. The sample was coated with a 10 nm gold layer prior to measurement.

Time-of-Flight Secondary Ion Mass Spectrometry: ToF-SIMS was performed on a ToF-SIMS[5] instrument (ION-TOF, Münster, Germany) equipped with a Bi liquid metal primary ion source and a nonlinear time-of-flight analyzer. For chemical surface characterization the Bi source was operated in the "bunched" mode, providing 0.7 ns Bi^+ ion pulses at 25 keV energy and a lateral resolution of ≈4 µm. Negative polarity spectra were calibrated on the C^-, CH^-, and CH_2^- peaks. Primary ion doses for spectrometry were kept below 10^{11} ions cm^{-2} (static SIMS limit). After having established the chemical assignments from spectrometry data and the structures precisely aligned to the primary beam, high lateral resolution (3D) images were obtained applying the "burst alignment" mode of the primary ion source. This mode avoids chromatic aberration of the Bi primary ion beam and therefore provides a highly focused ion beam allowing for sub-µm lateral resolutions. Charge compensation was achieved by applying an electron flood gun providing electrons of 21 eV and tuning the secondary ion reflectron accordingly.

Direct Laser Writing Experiments: Direct laser writing experiments were performed using a commercially available DLW system (Photonic Professional GT, Nanoscribe GmbH, Germany) equipped with an frequency doubled Erbium fiber laser with a 780 nm center wavelength and a pulse duration of close to 90 fs and a Zeiss Plan-Apochromat 63x/1.4 Oil DIC objective. 3D patterning was performed by laser scanning via a set of galvo-mirrors and mechanical stages. All procedures were conducted in Dip-in DLW mode.

Photoresist Preparation: Compound **1** (1.00 g, 1.08 mmol, 1 eq), compound **2** (1.05 g, 2.16 mmol, 2 eq), and DETC (5 mg, 0.25%wt) were added to a 5 mL brown glass vial equipped with a stir bar. The solution was stirred overnight at ambient (yellow light) conditions.

Preparation of Glass Substrates: Glass substrates were reacted with 3-(trimethoxysilyl)propyl methacrylate prior to usage via a literature procedure.[27]

DLW of Cuboid Structures: Silanized glass substrates with a dimension of 22 mm × 22 mm × 0.17 mm were used. The photoresist was drop casted onto the substrate. The scan raster was set to be 0.3 µm laterally and 0.5 µm axially. Development of the sample was conducted via a literature procedure.[27]

DLW of Woodpile Photonic Crystals and Cubic Unit Cells: Silanized DiLL glass substrates (Nanoscribe GmbH, Germany) with a dimension of 25 × 25 × 0.7 mm were used. The photoresist was drop casted onto the substrate. Development of the sample was conducted in acetone (30 min) followed by critical point drying in order to avoid capillary forces that occur during the conventional drying procedure. For cubic unit cells: the axial scan raster was chosen to be 0.5 µm. For woodpiles: each line was subsequently exposed five times in order to reduce structure deformation.

Thiol-Michael Postmodification Reaction: To a glass vial 2-bromo-2-methyl propionic acid 2-(3,5-dioxo-10-oxa-4-azatricyclo[5.2.1.02,6]dec-8-en-4-yl) ethyl ester (5.8 mg, 2×10^{-5} mol), dichloromethane (DCM) (20 mL), and triethylamine (0.04 mL) were added. Into this solution, a substrate containing cuboid structures was immersed followed by a 24 h period of slow shaking using a lab scale platform shaker. Afterward the substrate was subsequently developed in DCM (20 min), acetone (5 min), and water (5 min).

Copper-Catalyzed Azide-Alkyne Cycloaddition Postmodification Reaction: A glass vial was loaded with CuI (4.3 mg, 3×10^{-5} mol), DMF (30 mL), PMDETA (6.3 µL, 3×10^{-5} mol), PEG-N_3 (6 mg, 3×10^{-6} mol) and a 2 mm stir bar. Into this solution, a substrate containing cuboid structures was immersed followed by a 48 h period of slow stirring (without the stir bar touching the substrate). Afterward the substrate was subsequently developed in DMF (20 min) and water (5 min). In order to prevent grease/oil contamination while ensuring absence of oxygen, the procedure (excluding the development steps) was performed under inert atmosphere in a glove-box. For postmodification using 2-azidoethyl 2-chloropropanoate, CuCl, PMDETA, and DMF were employed.

Supporting Information

Supporting Information is available from the Wiley Online Library or from the author.

Acknowledgements

The study was supported by the Programme of Project Based Personal Exchange ASCR-DAAD (no. 14/08), by the Grant Agency of the Czech Republic (GACR) under Contract No. 15-09368Y, by the German Academic Exchange Service (facilitating a visit of A.S.Q. to the laboratories of C.R.-E.), by the project "BIOCEV—Biotechnology and Biomedicine Centre of the Academy of Sciences and Charles University" (CZ.1.05/1.1.00/02.0109), by the European Regional Development Fund as well as by the Karlsruhe Nano Micro Facility (KNMF), a Helmholtz Research Infrastructure at KIT. M.W. acknowledges support by the Karlsruhe Institute of Technology (KIT) through the Deutsche Förderungsgesellschaft (DFG) and the Center for Functional Nanostructures (CFN). C.B.-K. acknowledges continued funding via the STN program of the Helmholtz association and the Karlsruhe Institute of Technology (KIT) funding this project. The authors further acknowledge Patrice Brenner for performing FIB, Martin Schumann for SEM analysis, and Johannes Kaschke for discussions concerning photonic crystals.

Received: February 17, 2015
Revised: March 27, 2015
Published online: May 15, 2015

[1] Z. Nie, W. Li, M. Seo, S. Xu, E. Kumacheva, *J. Am. Chem. Soc.* **2006**, *128*, 9408.
[2] M. E. Helgeson, S. C. Chapin, P. S. Doyle, *Curr. Opin. Colloid Interface Sci.* **2011**, *16*, 106.

[3] R. Hao, R. Xing, Z. Xu, Y. Hou, S. Gao, S. Sun, *Adv. Mater.* **2010**, *22*, 2729.
[4] Y. Habibi, L. A. Lucia, O. J. Rojas, *Chem. Rev.* **2010**, *110*, 3479.
[5] S. M. George, *Chem. Rev.* **2009**, *110*, 111.
[6] J. C. Love, L. A. Estroff, J. K. Kriebel, R. G. Nuzzo, G. M. Whitesides, *Chem. Rev.* **2005**, *105*, 1103.
[7] L. J. Guo, *Adv. Mater.* **2007**, *19*, 495.
[8] Y. Chen, A. Pépin, *Electrophoresis* **2001**, *22*, 187.
[9] G. Subramania, Y.-J. Lee, I. Brener, T.-S. Luk, P. G. Clem, *Opt. Express* **2007**, *15*, 13049.
[10] C. N. LaFratta, J. T. Fourkas, T. Baldacchini, R. A. Farrer, *Angew. Chem. Int. Ed.* **2007**, *46*, 6238.
[11] S. Maruo, J. T. Fourkas, *Laser Photonics Rev.* **2008**, *2*, 100.
[12] M. Malinauskas, M. Farsari, A. Piskarskas, S. Juodkazis, *Phys. Rep.* **2013**, *533*, 1.
[13] S. H. Park, D. Y. Yang, K. S. Lee, *Laser Photonics Rev.* **2009**, *3*, 1.
[14] Z.-P. Liu, Y. Li, Y.-F. Xiao, B.-B. Li, X.-F. Jiang, Y. Qin, X.-B. Feng, H. Yang, Q. Gong, *Appl. Phys. Lett.* **2010**, *97*, 211105.
[15] B.-B. Xu, Y.-L. Zhang, H. Xia, W.-F. Dong, H. Ding, H.-B. Sun, *Lab Chip* **2013**, *13*, 1677.
[16] A. C. Scheiwe, S. C. Frank, T. J. Autenrieth, M. Bastmeyer, M. Wegener, *Biomaterials* **2015**, *44*, 186.
[17] A. Frölich, J. Fischer, T. Zebrowski, K. Busch, M. Wegener, *Adv. Mater.* **2013**, *25*, 3588.
[18] T. Bückmann, M. Thiel, M. Kadic, R. Schittny, M. Wegener, *Nat. Commun.* **2014**, *5*, 4130.
[19] J. Serbin, A. Ovsianikov, B. Chichkov, *Opt. Express* **2004**, *12*, 5221.
[20] J. Fischer, J. B. Mueller, J. Kaschke, T. J. A. Wolf, A.-N. Unterreiner, M. Wegener, *Opt. Express* **2013**, *21*, 26244.
[21] A. M. Greiner, M. Jäckel, A. C. Scheiwe, D. R. Stamow, T. J. Autenrieth, J. Lahann, C. M. Franz, M. Bastmeyer, *Biomaterials* **2014**, *35*, 611.
[22] T. Bückmann, N. Stenger, M. Kadic, J. Kaschke, A. Frölich, T. Kennerknecht, C. Eberl, M. Thiel, M. Wegener, *Adv. Mater.* **2012**, *24*, 2710.
[23] H. C. Kolb, M. G. Finn, K. B. Sharpless, *Angew. Chem. Int. Ed.* **2001**, *40*, 2004.
[24] A. Ovsianikov, J. Viertl, B. Chichkov, M. Oubaha, B. MacCraith, I. Sakellari, A. Giakoumaki, D. Gray, M. Vamvakaki, M. Farsari, C. Fotakis, *ACS Nano* **2008**, *2*, 2257.
[25] B. Richter, T. Pauloehrl, J. Kaschke, D. Fichtner, J. Fischer, A. M. Greiner, D. Wedlich, M. Wegener, G. Delaittre, C. Barner-Kowollik, M. Bastmeyer, *Adv. Mater.* **2013**, *25*, 6117.
[26] B. J. Adzima, C. J. Kloxin, C. A. DeForest, K. S. Anseth, C. N. Bowman, *Macromol. Rapid Commun.* **2012**, *33*, 2092.
[27] A. S. Quick, J. Fischer, B. Richter, T. Pauloehrl, V. Trouillet, M. Wegener, C. Barner-Kowollik, *Macromol. Rapid Commun.* **2013**, *34*, 335.
[28] A. S. Quick, H. Rothfuss, A. Welle, B. Richter, J. Fischer, M. Wegener, C. Barner-Kowollik, *Adv. Funct. Mater.* **2014**, *24*, 3571.
[29] A. Massi, D. Nanni, *Org. Biomol. Chem.* **2012**, *10*, 3791.
[30] B. Yao, J. Sun, A. Qin, B. Tang, *Chin. Sci. Bull.* **2013**, *58*, 2711.
[31] C. E. Hoyle, A. B. Lowe, C. N. Bowman, *Chem. Soc. Rev.* **2010**, *39*, 1355.
[32] B. D. Fairbanks, T. F. Scott, C. J. Kloxin, K. S. Anseth, C. N. Bowman, *Macromolecules* **2008**, *42*, 211.
[33] J. W. Chan, J. Shin, C. E. Hoyle, C. N. Bowman, A. B. Lowe, *Macromolecules* **2010**, *43*, 4937.
[34] J. W. Chan, H. Zhou, C. E. Hoyle, A. B. Lowe, *Chem. Mater.* **2009**, *21*, 1579.
[35] B. D. Fairbanks, E. A. Sims, K. S. Anseth, C. N. Bowman, *Macromolecules* **2010**, *43*, 4113.
[36] K. M. Ho, C. T. Chan, C. M. Soukoulis, R. Biswas, M. Sigalas, *Solid State Commun.* **1994**, *89*, 413.
[37] P. Mueller, M. Thiel, M. Wegener, *Opt. Lett.* **2014**, *39*, 6847.
[38] J. Fischer, M. Wegener, *Laser Photonics Rev.* **2012**, *7*, 22.
[39] T. F. Scott, B. A. Kowalski, A. C. Sullivan, C. N. Bowman, R. R. McLeod, *Science* **2009**, *324*, 913.
[40] M. Hesse, H. Meier, B. Zeeh, *Spectroscopic Methods in Organic Chemistry*, 2nd ed., Thieme, Stuttgart **2007**.
[41] J. W. Chan, C. E. Hoyle, A. B. Lowe, *J. Am. Chem. Soc.* **2009**, *131*, 5751.
[42] G. Mantovani, F. Lecolley, L. Tao, D. M. Haddleton, J. Clerx, J. J. L. M. Cornelissen, K. Velonia, *J. Am. Chem. Soc.* **2005**, *127*, 2966.
[43] X. Tao, Z. Gao, T. Satoh, Y. Cui, T. Kakuchi, Q. Duan, *Polym. Chem.* **2011**, *2*, 2068.